Metal clusters : theoretical approaches

M. Brack

METAL CLUSTERS: THEORETICAL APPROACHES

M. Brack

Institut für Theoretische Physik, Universität, D-8400 Regensburg, W-Germany

Résumé

Nous présentons une petite revue des méthodes théoriques utilisées pour la description des agrégats métalliques. En particulier, nous discutons du modèle autoconsistant du "jellium" dans le cadre de la théorie des fonctionnelles de densité et de quelques résultats récents concernant la structure des "super-couches" dans les agrégats de sodium.

Abstract

We present a brief review of the theoretical concepts used for the description of metal clusters. In particular, we discuss the selfconsistent jellium model within the framework of density functional theory and some recent results on the super-shell structure in Na clusters.

1. INTRODUCTION

It cannot be the aim of these lectures to give a detailed account of *all* theoretical aspects of metallic clusters. This would be a truly interdisciplinary task, involving quantum chemistry, molecular dynamics, atomic, molecular and solid state physics, and many aspects of nuclear physics as well. For the more phenomenological models used in cluster physics, we refer to the review article by de Heer *et al.* (1987b). A more detailed description of the selfconsistent theories discussed below, as well as a review of experimental results and their comparison with theory, will be found in a forthcoming article by de Heer and Brack (1992). The figures shown below as illustrations were taken from work in which the author was personally involved; they were selected purely for reasons of convenience.

We shall try, in Sec. 2, to give an overview of some of the facettes of the quantum many body problem given to us in the form of metal clusters, by going through a

series of successive approximations and simplifications used in various approaches, starting from purely microscopic quantal 'ab initio' descriptions and ending up with semiclassical mean field theory.

In the remaining part of these lectures we shall concentrate on the selfconsistent mean field approach. The most poweful tool here is the density functional theory (DFT) which is excessively used in cluster physics; we shall therefore devote Sec. 3 to a short presentation of the corresponding formalism.

Finally, in Sec. 4, we discuss the so-called selfconsistent jellium model for the description of metal clusters and present some selected results. Although this model greatly simplifies the physical situation by neglecting totally the geometric structure of the ions which make up the body of the clusters, it retains the quantal description of the valence electrons responsible for the shell structure, which is observed in many experiments and which bears so much resemblance to nuclear physics.

2. FROM THE QUANTAL MANY-BODY PROBLEM TO SEMICLASSICAL JELLIUM DROPS: A hierarchy of approximations

2.1) The quantal many body problem

Let us start by writing down the exact Hamiltonian for a neutral cluster consisting of N nuclei with Z electrons each:

$$\hat{H} = \sum_{\alpha=1}^{N}\left\{\frac{\mathbf{P}_\alpha^2}{2M} + \sum_{i=1}^{Z}\left(\frac{\mathbf{p}_{\alpha_i}^2}{2m} - \frac{Ze^2}{|\mathbf{r}_{\alpha_i} - \mathbf{R}_\alpha|}\right) + \frac{1}{2}\sum_{\beta=1}^{N}\left(\frac{(Ze)^2}{|\mathbf{R}_\alpha - \mathbf{R}_\beta|} + \sum_{i,j=1}^{Z}\frac{e^2}{|\mathbf{r}_{\alpha_i} - \mathbf{r}_{\beta_j}|}\right)\right\}, \tag{1}$$

where M, $\mathbf{P}_\alpha$, $\mathbf{R}_\alpha$ are the mass, momenta and coordinates, respectively, of the nuclei, and m, $\mathbf{p}_{\alpha_i}$, $\mathbf{r}_{\alpha_i}$ those of the electrons in the α-th nucleus. (Self interactions must be left out of the double sums.) This constitutes a system of $N(Z+1)$ charged particles interacting via the Coulomb forces. Although the Hamiltonian (1) is exactly known, it is impossible to solve the corresponding Schrödinger equation.

Luckily, the different scales of nuclear and electronic masses allow a rather sharp separation of their treatment: the motion of the nuclei may be treated classically (see Sec. 2.3) or neglected altogether (see Sec. 2.2), whereas the electrons must be treated quantum-mechanically since they lead to the all-dominant shell effects.

In simple metals such as alkalis and to some extent also in Ag, Al, etc., the delocalisation of the valence electrons allows a further separation: to treat only the

w valence electrons of each atom quantum-mechanically and to include the 'core electrons' with the nuclei into a compact ion of charge $+we$. The assumption: "atom = ion + w valence electrons" is quite good for simple metals, esp. alkalis, and provides the basis for the largest part of metal cluster calculations. The Hamiltonian then is reduced to that of N interacting ions ($\hat{H}_N$) and wN interacting electrons in an external field ($\hat{H}_{el}$):

$$\hat{H} = \hat{H}_N + \hat{H}_{el}, \tag{2}$$

with

$$\hat{H}_N = \sum_{\alpha=1}^{N} \left\{ \frac{\mathbf{P}_\alpha^2}{2M} + \frac{1}{2} \sum_{\beta(\neq\alpha)=1}^{N} \frac{(we)^2}{|\mathbf{R}_\alpha - \mathbf{R}_\beta|} \right\}, \tag{3}$$

$$\hat{H}_{el} = \sum_{i=1}^{wN} \left\{ \frac{\mathbf{P}_i^2}{2m} + V_I(\mathbf{r}_i) + \frac{1}{2} \sum_{j(\neq i)=1}^{wN} \frac{e^2}{|\mathbf{r}_i - \mathbf{r}_j|} \right\}, \tag{4}$$

where the ionic potential

$$V_I(\mathbf{r}) = -\sum_{\alpha=1}^{N} \frac{we^2}{|\mathbf{r} - \mathbf{R}_\alpha|}. \tag{5}$$

couples the electronic and ionic degrees of freedom. The effect of the core electrons is usually taken into account by replacing the pure Coulomb potential in (5) by a suitable pseudopotential, as is has been done successfully in solid state theory (see, e.g., Ashcroft and Mermin, 1976):

$$V_I(\mathbf{r}) = \sum_{\alpha=1}^{N} V_{ps}(|\mathbf{r} - \mathbf{R}_\alpha|). \tag{6}$$

Even if the nuclear part of $\hat{H}$ is ignored or treated by classical equations of motion (Sect. 2.3), the electron-electron interactions in (1) or (4) constitute an unsolvable many body problem. The most common solution for dealing with it is the *mean field* approximation: The wavefunctions of the electrons are taken to be those of non-interacting particles, i.e. Slater determinants. Determining them by an energy variation principle leads to the familiar Hartree-Fock (HF) approximation (see the lectures of J.-F. Berger). Hereby the average part of the electronic repulsion is included in a mean field or potential which, due to the finite range of the Coulomb interaction, is *nonlocal*. Extensions of the HF approximation are obtained by inclusion of (many) particle - (many) hole excitations in perturbation theory ('configuration mixing' and interaction).

An alternative version of the mean field approach is obtained from density functional theory in which correlations — also exchange contributions going beyond the HF approximation — can be included approximately in a *local* mean field (see Sec. 3). Both versions of mean field theory have been widely used for many-fermion systems in all branches of physics.

The mean-field concept explains most of the electronic shell effects and many other properties of metallic clusters, at least semi-quantitatively, and will be futher sketched in Secs. 2.4 - 2.5 below.

2.2) 'Ab initio' quantum chemistry

The ambitious goal of the quantum chemical 'ab initio' approach is to treat all the electronic degrees of freedom in (1) fully quantum-mechanically. This can only be done at the cost of 'freezing' the positions $\mathbf{R}_\alpha$ of all nuclei. The Born-Oppenheimer approximation then is used to vary adiabatically the positions of the nuclei, letting the electrons adjust their motion at any time to the momentaneous external field of the nuclei. Since the quantal many-electron problem is still too complicated, one starts from the Hartree-Fock approximation for the electronic wavefunctions and then treats their correlations perturbatively in a hierarchy of n-particle-n-hole configuration interactions. This approach is, for practical reasons, limited to small clusters (N up to about 20) and to a strict T=0 treatment; no zero point motion of the nuclei is included. (See a recent review article of Koutecky *et al.*, 1991, on this subject.)

2.3) Molecular dynamics and simulated annealing

The 'molecular dynamics' method is more ambitious in one point: to include the dynamics of the nuclei by solving their classical equations of motion. The price to pay is that the electrons cannot all be treated quantum-mechanically. Usually, they are treated in density functional theory (see Sect. 3). Car and Parrinello (1985) formulated a theory which couples the classical Newton equations for the nuclei to the quantum-mechanical Kohn-Sham equations of the electrons. In the applications to metal clusters, a further simplification is made by only treating the valence electrons explicitly, i.e., by using the electronic Hamiltonian (4) above. In this method, finite temperature effects can be included (Andreoni, 1991).

Often, however, a finite temperature is only used to allow the system to relax into the lowest minimum of its total energy and to determine in this way the optimal

ground state configuration. This is usually achieved by the 'simulated annealing' technique (Kirkpatrick *et al.*, 1983). A slightly modified version of this technique was used by Manninen (1986) to calculate for the first time the structure of small Na clusters with $N \leq 8$.

Small Al clusters with N up to 10 have recently been calculated by Jones (1991) and a series of small Na clusters ($N \leq 10$) by Röthlisberger and Andreoni (1991). The results obtained so far by the molecular dynamics method for the ground-state geometry of metal clusters are not much different from those found in the quantum-chemical 'ab initio' calculations.

2.4) Static mean field models

The next step is to ignore totally the motion of the nuclei, using only the electronic Hamiltoian (4) — including, eventually, the potential energy part of (3) — and treating Coulomb exchange and correlations of the electrons in density functional theory. This represents the static limit of molecular dynamics. The ionic structure is represented by the external potential V_I (5) or a corresponding pseudopotential (6).

The solution of this mean field problem still requires a fully 3-dimensional solution of the electronic Kohn-Sham equations; the optimal geometry of the ions entering the potential V_I must hereby be guessed. Several kinds of simplification have been used in order to avoid, on one hand, the systematic search of the ground state geometry — which would lead back to some form of molecular dynamics — and, on the other hand, the difficulties of solving a 3-dimensional Schrödinger equation; mostly, a spherical symmetry of the system was imposed (see, e.g., Iñiguez *et al.*, 1989).

The most dramatic and efficient simplification is to average out totally the ionic structure, replacing the charge distribution of the ions by a constant background charge in a finite (spherical or deformed) volume. This is the 3-dimensional, finite-size version of the *jellium model* which has already long ago been successfully used for the description of metallic bulk and surfaces properties (Lang and Kohn, 1970 - 1973).

The total neglect of the ionic structure is more justified than one perhaps might think at first sight: the pseudopotentials have no singularities and their sum in V_I is, indeed, a rather smooth function. This is the combined effect of screening and the Pauli principle, coming from the inner core electrons which fill the lowest orbitals in

the Coulomb-like potentials of the individual nuclei. We refer to textbooks on solid state phyics (see, e.g., Ashcroft and Mermin, 1976) for a more detailed discussion.

For finite clusters a wealth of papers, initiated by Ekardt (1984) and Beck (1984), has shown that a selfconsistent and essentially parameter-free microscopic jellium model calculation can account qualitatively, and in many cases even quantitatively, for many experimentally observed properties of metal clusters, in particular those of alkali metals (see also the lectures of S. Bjørnholm). Deformation (axial or triaxial) of the jellium background or a finite temperature of the electrons can be included at reasonable cost in the jellium model. Some of these calculations will be reviewed in Sec. 4.

The justification of the jellium model for the description of microclusters is, and will remain, an object of much debate and research. However, its undoubted virtue is that it can be applied also to large clusters with many hundreds or thousands of atoms, where the more structural models cannot be applied for practical reasons. The most beautiful example is the correct explanation of shells and supershells in large alkali clusters which will be given further account in Sec. 4.4.

2.5) Semiclassical and classical approaches

One more simplification can be made which leads to a considerable gain of efficiency in treating very large systems: the neglect of shell effects. This is done automatically by the explicit use of semiclassical approximations to the kinetic energy functional $\tau[\rho]$. The density functional formalism can then be exploited for direct density variational calculations: one no longer varies many electronic single-particle wavefunctions, but one single function, the electronic density $\rho(\mathbf{r})$ (or, if relevant, two spin densities). Hereby the single-particle structure, and with it the shell effects, are sacrified. But the advantage is an enormous gain in simplicity and calculational speed, and still such a model gives interesting results of average properties of the considered system. The famous prototype of such a model is the Thomas-Fermi (TF) model of the atom.

Extensions of the TF model (TFWDG, ETF,...) have been developed since long ago and been successfully used for finite fermion systems in many branches of physics. The variation of the density $\rho(\mathbf{r})$ can either be done exactly, leading to an Euler-Lagrange type (integro-)differential equation, or in restricted variational spaces using

trial density functions. In fact, the first selfconsistent jellium model calculations for spherical metallic clusters have been done using such a semiclassical density variational method by Cini (1975). Later semiclassical calculations have been done by Snider and Sorbello (1983), Brack (1989), Serra *et al.* (1989, 1990) and by Engel and Perdew (1991).

Many average properties of metal clusters can be described in such density variational calculations. A more formal and fundamental interest of this approach is the possibilty to connect the microscopic models to purely classical ones. In the large-N limit, the clusters behave like classical spheres or liquid droplets; this transition can, indeed, be quantitatively persued. In fact, a systematic 'leptodermous' expansion (see Myers and Swiatecki, 1969, for the nuclear case) of the semiclassical density variational results for spherical clusters allows for a selfconsistent determination of their surface and curvature energies, leading to the selfconsistent foundation of a classical liquid drop model, as it has been done in nuclear physics. Likewise, the asymptotic behaviour of electronic ionization potentials and affinities and their classical limits, which have recieved much attention in the literature, can be studied rigorously using this technique (see, e.g., Seidl *et al.*, 1991, and the literature quoted therein). Also, the collective multipole excitation frequencies obtained in a random phase (RPA) description can be shown in the classical limit (Brack, 1989) to go over to the so-called surface plasmon frequencies calculated by Mie (1908) (see also Sec. 4.2 and Fig. 2 below).

3. DENSITY FUNCTIONAL THEORY

We start from the Hamiltonian of a system of Z electrons moving in an external potential $V_{ext}(\mathbf{r})$ and interacting through the Coulomb forces:

$$\hat{H} = \sum_{i=1}^{Z} \left\{ \frac{\mathbf{p}_i^2}{2m} + V_{ext}(\mathbf{r}_i) + \frac{1}{2} \sum_{j(\neq i)=1}^{Z} \frac{e^2}{|\mathbf{r}_i - \mathbf{r}_j|} \right\} . \tag{7}$$

The exact wavefunction $\Psi(\mathbf{r}_1, \mathbf{r}_2, ..., \mathbf{r}_Z)$ belonging to this Hamiltonian can in general not be calculated. From it we define the one-body density matrix[1] $\rho_1(\mathbf{r}', \mathbf{r})$:

$$\rho_1(\mathbf{r}', \mathbf{r}) = \int d^3r_2 \int d^3r_3 \, ... \int d^3r_z \, \Psi^*(\mathbf{r}', \mathbf{r}_2, ..., \mathbf{r}_z) \, \Psi(\mathbf{r}, \mathbf{r}_2, ..., \mathbf{r}_z) \, . \tag{8}$$

[1] For the sake of simpliciy, and since they will not really be needed here, we do not exhibit the spin degrees of freedom.

Its diagonal part is the density $\rho(\mathbf{r})$ which shall be normalized to the number Z of electrons:

$$\rho(\mathbf{r}) = \rho_1(\mathbf{r},\mathbf{r}) , \qquad \int \rho(\mathbf{r})\, d^3r = Z . \tag{9}$$

In both Hartree-Fock (HF) theory and density functional theory, the density $\rho(\mathbf{r})$ is written in terms of single-particle wavefunctions $\varphi_i(\mathbf{r})$:

$$\rho(\mathbf{r}) = \sum_{i=1}^{Z} |\varphi_i(\mathbf{r})|^2 . \tag{10}$$

In HF theory the ground-state wavefunction of the Z-body system is approximated by a Slater determinant Φ built from a complete set $\{\varphi_\alpha(\mathbf{r})\}$ of single-particle wavefunctions:

$$\Phi(\mathbf{r}_1, \mathbf{r}_2, ..., \mathbf{r}_z) = \det |\varphi_i(\mathbf{r}_j)|_{\,i,j=1,2,...Z} . \tag{11}$$

The density matrix (8) then takes the form

$$\rho_1(\mathbf{r}', \mathbf{r}) = \sum_{i=1}^{Z} \varphi_i^*(\mathbf{r}')\varphi_i(\mathbf{r}) , \tag{12}$$

from which Eq. (10) follows. The choice of the single-particle wavefunctions φ_i is governed by a variational principle: One makes the expectation value of the total Hamiltonian (7) between the Slater determinants (11) stationary with respect to the wavefunctions φ_i, subject to the condition of their orthogonalization by means of Lagrange multipliers ε_i. This leads to the so-called HF equations which are discussed extensively in J.-F. Berger's lectures.

Density functional theory (DFT) goes beyond the HF approach in that correlations are taken into account which are not contained in the HF energy — however, at the cost of an approximate treatment of the Coulomb exchange terms. The basic idea of DFT is almost as old as quantum mechanics and has already been used by Thomas (1927) and Fermi (1928) in their famous work: to calculate the total energy of a system by an integral over an expression depending only on the local density $\rho(\mathbf{r})$:

$$E_{tot} = \int \mathcal{E}[\rho(\mathbf{r})]\, d^3r = E[\rho] . \tag{13}$$

Mathematically speaking, the energy is assumed to be a functional of the local density $\rho(\mathbf{r})$, denoted by $E[\rho]$. The formal basis of the ensuing theory was laid by Hohenberg and Kohn (1964) in their famous theorem which they proved for a non-degenerate

electronic system. A more general proof, independent of ground-state degeneracy and of the so-called V-representability assumed by Hohenberg and Kohn, was given by Levy (1989) for this theorem which states that *the exact ground-state energy of a correlated electron system is a functional of the local density* $\rho(\mathbf{r})$, and that this functional has its variational minimum when evaluated for the exact ground-state density. This means that, ideally, the variational equation

$$\frac{\delta}{\delta\rho(\mathbf{r})}\left[E[\rho(\mathbf{r})] - \lambda\int\rho(\mathbf{r})\,d^3r\right] = 0\,, \tag{14}$$

using the Lagrange multiplier λ to fix the number of particles according to (9), would lead to the knowledge of the exact ground-state energy and density — if the exact functional $E[\rho]$ were known (which, alas, it is not).

We do not need to go into further details about this basic theorem and the general formalism of DFT, since this is the subject of many excellent reviews. [For a recent review on DFT and its applications in atomic, molecular and solid state physics, see Jones and Gunnarsson (1989); further reviews are quoted therein.] For further reference, let us just sketch the main steps and list the most important formulae. The usual way to break up the energy functional (13) for the Hamiltonian given by Eq. (7) is:

$$E[\rho] = T_s[\rho] + \int\left\{V_{ext}(\mathbf{r})\rho(\mathbf{r}) + \frac{1}{2}V_H[\rho(\mathbf{r})]\right\}d^3r + E_{xc}[\rho]\,. \tag{15}$$

Hereby $T_s[\rho]$ contains that part of the kinetic energy which corresponds to a system of *independent* particles with density ρ, and $V_H(\mathbf{r})$ is the Hartree (or direct, or classical) Coulomb potential

$$V_H(\mathbf{r}) = e^2\int\frac{\rho(\mathbf{r}')}{|\mathbf{r}-\mathbf{r}'|}\,d^3r'. \tag{16}$$

The last term in (15) is the so-called *exchange-correlation energy*; it contains the exchange part of the Coulomb energy plus all the contributions due to the other correlations (hereby also a correlation part of the kinetic energy), i.e. due to the fact that the exact wavefunction is not a Slater determinant.

$E_{xc}[\rho]$ is not known exactly for any finite interacting fermion system, and it is a matter of state-of-the-art of DFT to use more or less fancy approximations to it. The same holds for the kinetic energy functional $T_s[\rho]$ which is not known explicitly for many-fermion systems. The approximations derived from the Thomas-Fermi model

and its extensions (ETF etc.) allow to perform the direct density variation (14), as briefly sketched in Sec. 2.5 above.

In order to avoid the difficulty of finding an explicit density functional for the kinetic energy, Kohn and Sham (1965) proposed to write the density $\rho(\mathbf{r})$ in the form of Eq. (10) in terms of some trial single-particle wavefunctions $\varphi_i(\mathbf{r})$. This is, in fact, possible for any realistic, non-negative normalizable density (Gilbert, 1975). The non-interacting part of the kinetic energy density $\tau(\mathbf{r})$ can then be given in the form

$$\tau(\mathbf{r}) = \sum_{i=1}^{Z} |\nabla \varphi_i(\mathbf{r})|^2 \tag{17}$$

in terms of the same $\varphi_i(\mathbf{r})$. The variation (14) of the energy functional can now be done through a variation of the trial functions $\varphi_i(\mathbf{r})$ with a constraint on their norms like in the HF method, except that the HF ground-state energy $\langle \Phi | \hat{H} | \Phi \rangle$ here is replaced by $E[\rho]$ (15). This leads to the Kohn-Sham (KS) equations

$$\left\{ \hat{T} + V_{KS}(\mathbf{r}) \right\} \varphi_i(\mathbf{r}) = \varepsilon_i \varphi_i(\mathbf{r}) \tag{18}$$

in which the *local* potential $V_{KS}(\mathbf{r})$ is a sum of three terms:

$$V_{KS}(\mathbf{r}) = V_{KS}[\rho(\mathbf{r})] = V_{ext}(\mathbf{r}) + V_H[\rho(\mathbf{r})] + V_{xc}[\rho(\mathbf{r})] \; . \tag{19}$$

The first two parts are clear from above; the third term is the variational derivative of the exchange-correlation energy:

$$V_{xc}[\rho(\mathbf{r})] = \frac{\delta}{\delta \rho(\mathbf{r})} E_{xc}[\rho] \; . \tag{20}$$

Since both V_H and V_{xc} depend on the density, the KS equations (18) are nonlinear and must be solved selfconsistently; this is usually done iteratively like in the HF method. The important difference, however, is that the potential $V_{KS}(\mathbf{r})$ is *local* and the KS equations therefore are much easier to solve.

A remark is necessary concerning the interpretation of the wavefunctions $\varphi_i(\mathbf{r})$ and the energies ε_i obtained from the KS equations: they do *not* have the same physical meaning as in HF theory. The ansatz (10) for the density does *not* imply that the total wavefunction of the system here is taken to be a Slater determinant. In fact, one does not know the total wavefunction in DFT; the wavefunctions $\varphi_i(\mathbf{r})$ are just a variational tool to obtain an approximated ground-state density. Likewise, the ε_i do

not, in general, have the meaning of single-particle energies. An exception is made by the energies of the highest occupied KS level (ε_{HO}) and the lowest unoccupied KS level (ε_{LU}) on either side of the Fermi energy: they can be used to estimate ionization potentials and electron affinities, respectively (see, e.g., Levy and Perdew, 1985, and references quoted therein).

The DFT can easily be extended to take the electron spin explicitly into account by introducing a spin-up density and a spin-down density. This leads, instead of (18), to two coupled equations for the two spin densities. Since there is no need, so far, to make use of this spin density formalism for metallic clusters, we refer to the literature for further details (see, e.g., Jones and Gunnarsson, 1989; Dreizler and Gross, 1990).

Another extension of DFT concerns the inclusion of a finite temperature $T > 0$ of the electrons. Mermin (1965) derived the Hohenberg-Kohn theorem and the Kohn-Sham formalism at $T > 0$ for a grand canonical system of electrons. Later Evans (1979) showed that the DFT also applies to canonical systems. In essence, one goes over from the (internal) energy $E[\rho]$ (15) of the system to the *free energy* $F[\rho]$:

$$F[\rho] = E[\rho] - TS_s[\rho] \,, \tag{21}$$

where S_s is noninteracting part of the entropy. The exchange-correlation energy $E_{xc}[\rho]$ will, in general, depend explicitly on T (i.e., not only through the density). The Kohn-Sham formalism then is obtained by including into the definition of the densities (10,17) the finite-temperature occupation numbers n_i:

$$\rho(\mathbf{r}) = \sum_i |\varphi_i(\mathbf{r})|^2 n_i \,, \qquad \tau(\mathbf{r}) = \sum_i |\nabla\varphi_i(\mathbf{r})|^2 n_i \,, \qquad \sum_i n_i = N \tag{22}$$

and by minimizing $F[\rho]$ with respect to both the φ_i and the n_i. Since S_s does not depend explicitly on the wavefunctions φ_i, their variation gives exactly the same form (18) of the KS equations, the only difference being that the potential V_{KS} becomes temperature dependent. Variation of the n_i gives their explicit form in terms of the ε_i; the result depends on whether one treats the system as a canonical or a grand canonical ensemble. (In the latter case, where the chemical potential μ is used to constrain the average particle number N, one obtains the familiar Fermi occupation numbers.) For an extensive discussion of the finite-temperature DFT and calculations, we refer to a review article by Gupta and Rajagopal (1982). Its application to metallic clusters is discussed in Sec. 4.4 below.

The Kohn-Sham approach is very appealing since, ideally, it allows to reduce the correlated many-body problem to the solution of a selfconsistent one-body problem of Hartree type. The reality is that only approximate functionals for the exchange-correlation part of the energy are at hand. The simplest and most frequently applied functionals for $E_{xc}[\rho]$ make use of the *local density approximation* (LDA): One performs more or less sophisticated many-body calculations for a hypothetical infinite system of electrons with constant density ρ, whereby the diverging Hartree energy is cancelled by embedding the electrons in a jellium-like background of opposite charge density. The resulting energy per electron is used to extract the corresponding xc-part $e_{xc}(\rho)$ which is a function of the variable ρ. The LDA for a finite system with variable density $\rho(\mathbf{r})$ then consists in assuming the local xc-energy density to be that of the corresponding system with density $\rho = \rho(\mathbf{r})$:

$$E_{xc}^{LDA}[\rho] = \int \rho(\mathbf{r}) e_{xc}(\rho(\mathbf{r}))\, d^3r \,. \tag{23}$$

By construction, this approximation is exact in those regions of space where the density $\rho(\mathbf{r})$ is constant, and it is badly justified where the density varies strongly, as e.g. in the surface region of metal clusters. In spite of its simplicity, the LDA in connection with the Kohn-Sham approach has met a considerable success in almost all branches of physics. (See, e.g., Jones and Gunnarsson, 1989, for its applications to electronic systems.) The extension to the spin density formalism is straightforward; it is usully termed 'local spin density' (LSD) formalism.

A lot of research has been done in going beyond the LDA and LSD schemes. Both gradient expansions and explicitly nonlocal forms of $E_{xc}[\rho]$ have been developed and extensively studied. They have, however, only occasionally been applied to metallic clusters and so far not appeared to bring significant improvements over results obtained with the LDA; we therefore refrain from discussing them explicitly here.

One serious break-down of the LDA concerns the asymptotic behaviour of the KS potential for Coulombic systems. In HF theory, where the Coulomb exchange is treated exactly, it is well-known that the mean field asymptotically falls off like $1/r$ far outside the surface of a spherical system; this is simply the field, seen by one electron which is taken far away, of the remaining spherical charge distribution. This is no longer so in the KS theory when the exchange is treated in local density ap-

proximation. In fact, the Hartree potential V_H (16) contains spurious self interaction contributions of the electrons which are exactly cancelled when the Fock potential is added to it. However, with the LDA one makes a crude approximation to the Fock potential, whereas the Hartree potential is left intact, so that this cancellation cannot take place. As a consequence, one obtains too much screening and the KS potential falls off much faster than $1/r$. A 'self interaction correction' (SIC), which restores the correct asymptotic behaviour of the KS potential, has therefore been introduced and tested for atomic systems (Perdew and Zunger, 1981). It makes, however, the KS potential state-dependent and thereby complicates the selfconsistent calculations appreciably.

We should point out here that the HF approach with zero-range forces, as it is widely used in nuclear physics with the Skyrme type effective interactions, is formally *identical* to the Kohn-Sham approach with a local spin density functional (except for a straightforward generalization to take effective masses into account). Having this and the Hohenberg-Kohn theorem in mind, one should be aware of the fact that correlations *are* contained in what is usually called the HF energy, albeit in an implicit way through the fit of the HF energy to physical nuclear masses.

The application of the KS method to atomic clusters becomes very complex with increasing number of atoms. The variation of the positions of all atoms and a simultaneous, fully selfconsistent treatment of all electrons in large clusters exceeds the capacities even of modern computers. For clusters consisting of simple metal atoms, in particular alakalis, one therefore exploits the approximate separability into one or a few valence electrons and an ionic core to restrict the degreees of freedom. The idea thus is to treat only the valence electrons explicitly by DFT as interacting particles in the *pseudopotentials* created by the ions. If the ionic structure is neglected altogether and replaced by a homogeneous, positive background density, one arrives at the *jellium model* wich has been surprisingly successful and will be discussed in the following section.

4. THE SELFCONSISTENT JELLIUM MODEL

4.1. Basic concepts

The basic idea of the selfconsistent jellium model is to replace the distribution of the ionic cores by a constant positive background or 'jellium' density[2] ρ_{I0} in a finite volume and to treat only the valence electrons explicitly in the mean field approximation, either microscopically as described in this section, or semiclassically (see Sec. 2.5). The jellium background may be either spherical, ellipsoidal or arbitrarily deformed.

Almost all jellium calculations so far have been performed within DFT. The total energy of the cluster is therefore expressed as a functional of the local electron density $\rho(\mathbf{r})$ by:

$$E[\rho] = T_s[\rho] + E_{xc}[\rho] + \int \left\{ V_J(\mathbf{r})\rho(\mathbf{r}) + \frac{1}{2}\rho(\mathbf{r}) \left[e^2 \int \frac{\rho(\mathbf{r}')}{|\mathbf{r}-\mathbf{r}'|}\, d^3r' \right] \right\} d^3r + E_J. \quad (24)$$

The notation here is as in Sec. 3 above; V_J and E_J are the potential and the total electrostatic energy, respectively, of the ionic jellium background. The energy E_J does not depend on the electron density but is included so that E represents the total binding energy of the cluster. The density $\rho(\mathbf{r})$ must be normalized to the number wN of valence electrons:

$$\int \rho(\mathbf{r})\, d^3r = wN, \quad (25)$$

where w is the valence factor (number of valence electrons per atom). By a variation of the energy $E[\rho]$ (24) with respect to the $\varphi_i^*(\mathbf{r})$, one then arrives at the Kohn-Sham equations (18,19) with $V_{ext}(\mathbf{r})$ replaced by the jellium potential $V_J(\mathbf{r})$.

Most applications of the jellium model to metal clusters so far were restricted to the *local density approximation* (LDA) for the exchange-correlation functional $E_{xc}[\rho]$. (For a recent Hartree-Fock calculation, see the remark at the end of Sec. 4.2 below.) Metal clusters (besides metal surfaces) present perhaps one of the most crucial testing grounds for the LDA, since their surfaces are typically much steeper than those of atoms or small molecules. However, the success of the LDA in conjuncion with the jellium model in describing surface energies and work functions for metal surfaces

[2]Throughout this paper, we denote by ρ the *particle* densities and not the charge densities. The charges (in multiples of e) appear explicitly in all formulae with their correct signs.

(Lang and Kohn, 1970, 1971; Monnier *et al.*, 1978) — at least of alakli-like metals — has encouraged, and some extent also justified, its application to metallic clusters.

One essential point of the jellium model is that it contains only one single parameter, namely the Wigner-Seitz radius r_s which characterizes the metal. It is related to the jellium density ρ_{I0} by

$$\rho_{I0} = \left(\frac{4\pi}{3} {r_s}^3\right)^{-1} . \tag{26}$$

Otherwise, the model is completely free of parameters since the electron density is determined variationally. Usually, one takes the bulk value for r_s corresponding to the ionic lattice in the crystal. This is, naturally, only justified for large clusters. In microclusters there is some weak experimental evidence for a decreasing density (i.e. an increase of the volume). In the jellium model we have, however, no way to determine the finite-size variation of r_s theoretically, so that the simplest choice is that of the bulk value.

A remark aout the internal consistency of the jellium model might be appropriate at this place. If we consider the inner part of a large neutral cluster and neglect the surface effects, the energy per electron $e(\rho)$ as a function of the (constant) density ρ is given by

$$e(\rho) = \kappa \rho^{2/3} + e_{xc}(\rho) , \tag{27}$$

where the first part is the kinetic energy per electron. The Coulomb energies cancel exactly if the density ρ is chosen to be equal to the jellium density ρ_{I0}, which must be done to ensure charge neutrality. If we now search for a minimum of $e(\rho)$ (27) with respect to varying ρ (and, with it, ρ_{I0}!), we find it for values $r_s \simeq 4$ - 4.3 a.u., depending somewhat on the detailed LDA xc-functional used. For the LDA functional of Gunnarsson and Lundqvist (1976), e.g., which has often been used for metal cluster calculations, this minimum is at $r_s = 4.08$ a.u. In such a variational calculation there is, of course, only one metal which has a stationary value of its density in the bulk region. It is perhaps no coincidence that the jellium model works best for alkali metals, in particular sodium, with r_s values close to this minimum.

A large majority of KS calculations so far has been performed assuming spherical symmetry of the clusters. The calculation then becomes one-dimensional and is relatively easy to do for not too large clusters. We shall briefly review these calculations in Sec. 4.2. In Sec. 4.3, calculations in two and three dimensions are discussed,

corresponding to axially and non-axially deformed clusters, respectively. Finally, in Sec. 4.4, we report on recent spherical calculations for very heavy clusters at finite temperatures, focusing especially on the so-called supershell structure.

4.2. Spherical jellium model

In the spherical jellium model, the ionic background density $\rho_I(r)$ is that of a uniformly charged sphere with radius R_I:

$$\rho_I(r) = \rho_{I0}\Theta(r - R_I), \qquad R_I = r_s N^{1/3}, \tag{28}$$

where the value of R_I is fixed by the number N of ions. The jellium potential $V_J(r)$, which replaces the sum of individual ionic potentials (5) or (6), and the energy E_J are then easy to evaluate and given by

$$V_J(r) = \begin{cases} -\frac{wNe^2}{2R_I}\left[3 - \left(\frac{r}{R_I}\right)^2\right] & \text{for} \quad r \le R_I \\ -\frac{wNe^2}{r} & \text{for} \quad r \ge R_I \end{cases}, \tag{29}$$

$$E_J = \frac{3}{5}\frac{(wNe)^2}{R_I}. \tag{30}$$

If the electron density is also assumed to have spherical symmetry, the total KS potential (19) is spherical and the single-particle states $\varphi_i(\mathbf{r})$ will have good angular momentum quantum numbers ℓ_i, m_i; their angular parts being given by $Y_{\ell_i m_i}(\theta, \phi)$ in polar coordinates (r, θ, ϕ). Eqs. (18) can then be reduced to radial Schrödinger equations for the radial parts $R_{n_i \ell_i}(r)$ of the wavefunctions and solved numerically on a one-dimensional mesh in the variable r. This was performed for the first time by Ekardt (1984a,b) and independently by Beck (1984a,b). As a variational, though not fully selfconsistent, precursor of this model we mention that of Martins *et al.* (1981), who replaced the selfconsistent KS potential (19) by a simple variational square-well potential. All these authors used LDA functionals for the exchange-correlation part of the energy.

Later on, many spherical KS calculations in the jellium model were performed by various groups. By way of an example, we mention here a recent review by Balbàs and Rubio (1991) which summarizes over 30 papers published by groups at Valladolid, Valencia and other spanish universities, encompassing also semiclassical density variational calculations and extensions of the jellium model. Some recent KS calculations for very large clusters will be reported in Sect. 4.4 below.

In Figure 1 we show as an illustration the density profile $\rho(r)$ and the total mean field $V(r)$ of the electrons for Na_{198}, obtained both microscopically (KS) and in semiclassical (ETF) density variational calculations.

Let us summarize briefly some of the main results and successes of the spherical jellium-KS calculations. (For more details, we refer the interested reader to the forthcoming review by de Heer and Brack, 1992.)

- Magic numbers for filled spherical major shells agree with few exceptions with the observed peaks in the mass abundance spectra (see also Sect. 4.4).

- Ionization potentials (IP) and electron affinities (EA) show a good overall behaviour; the jumps of the saw-teeth are usually at right places but often too large in absolute values. This is related to the bulk value of the work function W which is asymptotically reached in the $N \rightarrow \infty$ limit but comes out too large in the jellium model as well-known since Lang and Kohn (1970, 1971). (See Seidl *et al.*, 1991, for a discussion of the asymptotic slopes of IP and EA when plotted versus $1/R_I$.)

- The optical response of alkali clusters can qualitatively be well described by the jellium model in the framework of linear response theory (RPA or its equivalent, the so-called time-dependent local density approximation, TDLDA). Beck (1984b) was the first to calculate in this way static electric dipole polarisabilities and Ekardt (1984a, 1985a,b, 1986) obtained dynamical dipole polarisabilities in TDLDA. The RPA sum rule approach was used in semiclassical density variational calculations by Brack (1989) and also by Serra *et al.* (1989) for the description of the collective multipole excitations of the valence electrons, the so-called surface plasmons, with are the anologues of the nuclear isovector giant resonances. Figure 2 shows as an example the multipole frequencies, obtained for spherical clusters, and their asymptotic limits, the classical Mie frequencies (Mie, 1908). An approximation to the RPA based on local currents ("local RPA"), which is an extension of the usual sum rule approach and allows to obtain rather good RPA spectra from ground-state densities (!), has been developed by Brack (1989) and Reinhard *et al.* (1990). First microscopic RPA calculations for spherical alkali clusters were performed by Yannouleas *et al.* (1989); Bertsch (1990) wrote the first fully selfconsistent KS+RPA code using the spherical jellium model. All TDLDA or RPA results for the lowest, and most collective, dipole excitation energy are too high by about $10 - 15\%$ with respect to the experimental peak energies (de Heer *et al.*, 1987a; Bréchignac *et al.*, 1989; Selby *et al.*, 1991;

Tiggesbäumker *et al.*, 1991) which are systematically red-shifted with respect to the classical Mie plasmon (cf. also Fig. 2). This goes along with a too low theoretical dipole polarisability and is presumably the fault of the LDA which fails in the cluster surface. In the region $8 < N < 18$, several experiments show a clear splitting of the dipole peak which can only be explained by a static deformation of the corresponding clusters.

Finally, we draw attention to recent Hartree-Fock plus RPA calculations for spherical Na clusters up to $N = 92$ within the jellium model, where the Coulomb exchange is treated exactly but no further correlations are included, by Guet and Johnson (1991). Their dipole excitation spectra resemble very much those obtained in the KS + RPA calculations just mentioned; this seems to imply that the correlation part of the $E_{xc}[\rho]$ LDA functional does not contribute appreciably to the dipole response.

4.3. Deformed jellium model

Some of the shortcomings of the spherical jellium model can be removed, or at least reduced, by relaxing the spherical shape of the clusters. Indeed, there is good experimental evidence that clusters are deformed in regions between the major spherical shell closures: The phenomenological Clemenger-Nilsson model (see de Heer *et al.*, 1987b, for a discussion of this model which is just a copy of the famous Nilsson model for deformed nuclei) allows to interpret the fine structure of mass abundance spectra and the splitting of the surface plasmons of clusters in the mass regions $8 < N < 18$ and $20 < N < 40$ (Selby *et al.*, 1989, 1991; Tiggesbäumker *et al.*, 1991). In the Nilsson model, the potential depends on one or two deformation parameters, and the equilibrium (or ground state) shape of each cluster is calculated simply by minimizing the sum of occupied single-particle energies. Obviously, such a model is not selfconsistent in two respects: first, the density distribution of the electrons is not guaranteed to have the same shape as that of the potential (although this is approximately the case at the shapes of minimal total energy), and second, the sum of single-particle energies is far from being equal to the total binding energy of an interacting system.

It is therefore of a basic theoretical interest to verify the phenomenological potential of the Clemenger-Nilsson model by microscopic, selfconsistent calculations in the framework of density functional theory. Since in the jellium model there is no real

selfconsistency between the ionic background density and that of the electrons, this must be put in explicitly. In the deformed selfconsistent jellium model, one therefore has to assume that the ionic background density follows, on the average, the shape of the electrons. Practically, one parametrizes the deformed shape of the jellium density, lets the electrons adjust themselves in the corresponding deformed ionic potential (including their interaction and exchange-correlation effects in Kohn-Sham approximation, as usual), and then one minimizes the total energy with respect to the jellium shape. This is, or course, consistent with the spirit of the Born-Oppenheim approach used in quantum chemical and molecluar dynamics calculations (see Secs. 2.2, 2.3 above), except that the microscopic ionic structure here is averaged out. Allowing for axial or nonaxial shapes of the constant ionic background density, however, brings the jellium model one step closer to those more fundamental approaches in the sense that the average geometry of the ions can be varied.

One technical problem in the deformed jellium model is that the background jellium potential $V_J(\mathbf{r})$ is no longer a simple analytical function as in the spherical case, cf. Eq. (29). It must therefore be calculated numerically either by direct integration of the jellium density or by solving the Poisson equation. Similarly, the KS equations become more complex with decreasing symmetry of the cluster and have to be solved in two or three dimensions explicitly.

The existence of axially deformed equilibrium shapes within the framework of the selfconsistent jellium model has been confirmed in Kohn-Sham calculations for ellipsoidal clusters (Ekardt and Penzar, 1988, 1991; Penzar and Ekardt, 1990). These authors use an axially symmetric ellipsoidal jellium density with constant volume and half-axes z_0, ρ_0 given in terms of a single deformation parameter δ, restricted by $-2 < \delta < 2$, and the cluster radius R_I (28)

$$z_0 = \left(\frac{2+\delta}{2-\delta}\right)^{2/3} R_I \; ; \qquad \rho_0 = \left(\frac{2-\delta}{2+\delta}\right)^{1/3} R_I \; ; \tag{31}$$

The electronic density is assumed to have axial symmetry, too, and the Kohn-Sham equations are solved in spheroidal coordinates, using again the LDA functional of Gunnarsson and Lundqvist (1976) for the xc-energy. The total energy of the cluster must be calculated for each deformation δ, and the ground state is found by minimizing the resulting energy with respect to δ.

Results of this spheroidal model for IP's and EA's for sodium and copper clusters

(Ekardt and Penzar, 1988; Penzar and Ekardt, 1990) show that the shell structure in these quantities is appreciably reduced by the deformation effects and in reasonable agreement with experiment, but still somewhat exaggerated. Ekardt and Penzar (1991) also used their spheroidal model in TDLDA to calculate collective photoabsorption spectra of deformed clusters; as in the Clemenger-Nilsson model, the right order of magnitude of the splitting was found for the dipole peaks.

Triaxial deformations of small sodium clusters have recently been investigated in the selfconsistent KS framework by Lauritsch *et al.* (1991). Here, a triaxial elliposid with constant volume was assumed for the jellium density; the jellium density was given a diffuse surface with a width of approximately one atomic unit. The KS equations (in LDA) were then solved numerically on a three-dimensional mesh for each given deformation of the jellium background. Potential energy surfaces of these triaxially deformed clusters were presented as functions of the two Hill-Wheeler coordinates (β, γ) (Hill and Wheeler, 1953). Na_{12} was found to have its mimimum for a triaxial shape, as can be seen from Figure 3, whereas Na_{14} is predicted to be axial with a prolate minimum; this confirms the results of the Clemenger-Nilsson model. An interesting phenomenon in the results of Lauritsch *et al.* (1991) is the occurrence of serveral almost degenerate shape isomers with different spherical, axial or non-axial shapes, separated by barriers of $\sim$ 0.5 - 1 eV. This shape isomerism reminds, indeed, of that found in *ab initio* quantum chemical and molecular dynamics calculations.

4.4. Finite temperature calculations and supershells

In many experiments, clusters are produced at finite temperatures of up to several hundred Kelvin or even more (see the lectures by Bjørnholm). The manifestation of shell structure in the abundance spectra of cluster beam experiments is thought to be a result of evaporation of neutral atoms by the hot clusters: the closer the number of valence electrons gets to a magic number corresponding to a filled spherical shell, the more stable the cluster will be and the smaller the probability for evaporation of a further atom, so that finally, at the time of detection — when the beam has cooled off — the magic species are the most abundant.

The question therefore arizes to which extent a finite temperature affects the magnitude of the electronic shell effects themselves. It is well-known from nuclear physics, that large enough temperatures smear out the shell structure in a finite

fermion system (Bohr and Mottelson, 1975, Brack and Quentin, 1981). In particular, the observability of the so-called super-shell structure (Nishioka *et al.*, 1990) may become difficult due to these temperature effects.

At first sight one may think that even many hundred Kelvin are small on the scale of the electronic single-particle energies, so that their effect should be negligible. This is certainly true for microclusters with less than a hundred atoms, where the main spacing between electronic levels corresponds to several thousand Kelvin. However, in very large clusters in the mass region $N \gtrsim 1000-2000$, which now have become available in expansion sources, the spectra are much more compressed and the temperatures in question do have a noticeable effect. Furthermore, the detailed shape of the abundance spectra depends in a rather subtle way on the first and second differences of the total cluster (free) energies with respect to the atomic number, $\Delta_1 F(N)$ and $\Delta_2 F(N)$, respectivey, such that the temperature smearing effects can, indeed, become visible in the experimental results (Bjørnholm *et al.*, 1991).

These questions were addressed recently in finite-temperature Kohn-Sham-LDA calculations for sodium clusters in the spherical jellium model (Brack *et al.*, 1991a,b; Genzken and Brack, 1991). The electrons are treated as a canonical system in the heat bath of the ions; the canonical partition function is calculated exactly and from it, all relevant quantities such as the free energy, entropy and occupation numbers are derived selfconsistently. We refer to Brack *et al.* (1991b) for the details of these calculations and illustrate here the results with two figures.

A standard quantity for studying shell effects is the shell-correction energy

$$\delta F(N) = F(N) - \overline{F}(N)\,, \tag{32}$$

where $\overline{F}(N)$ is the *average* free energy of a cluster with N atoms. Here we have simply used a liquid drop model (LDM) expansion

$$\overline{F}(N) = F_{LDM}(N) = e_b N + a_s N^{2/3} + a_c N^{1/3}\,, \tag{33}$$

determining the surface energy a_s and the curvature energy a_c by a simple eye fit such that $\delta F(N)$ is oscillating around zero; this is done separately at each temperature. The bulk energy is fixed at its theoretical value e_b = -2.2567 eV, obtained for $r_s = 3.96$ a.u., independently of temperature.

The results for $\delta F(N)$ are plotted in Fig. 4 versus $N^{1/3}$ at the three temperatures $T = 0$ K, 400 K and 600 K. The magic numbers are given in the curve for $T = 0$ K

at the corresponding minima. The amplitude of the shell effects is clearly reduced with increasing temperature. Two minor shells in the transition region at $N = 506$ and $N = 638$, still visible at $T = 0$ K, are wiped out at $T > 0$. All other minima become less sharp than at $T = 0$.

The salient feature of the curves in Fig. 4 is the beating pattern of the otherwise quite regular shell structure. Such a pattern was shown by Balian and Bloch (1971) to be a very general feature of quantal eigenmodes in a cavity. The method of Balian and Bloch was applied to metal clusters by Nishioka *et al.* (1990) who termed the beating pattern "super-shells"; they used a phenomenological Woods-Saxon potential for the valence electrons.

The shell-correction energy $\delta F(N)$ is, however, not directly observable. As mentioned above, the mass abundances in expansion beams depend rather on the differences $\Delta_1 F(N)$ and $\Delta_2 F(N)$ which are even more sensitive to the temperature. In fact, these latter quantities were shown by Brack *et al.* (1991) to disappear completely for $N \gtrsim 600$ at temperatures $T \simeq 600$ K or above, putting in doubt the survival of the super-shell structure which only starts at $N \gtrsim 1000$.

In order to make the super-shells visible, nevertheless, Pedersen *et al.* (1991) proposed to scale up the mass yields by a factor depending exponentially on $N^{1/3}$. The temperature dependence of $\delta F(N)$ — and thus also of the differences $\Delta_1 F(N)$ and $\Delta_2 F(N)$ in which the average energies practically cancel — can be schematically estimated (Bohr and Mottelson, 1975) to go like

$$\delta F(T) = \delta F(0)\,\frac{t}{\mathrm{Sinh}t}\,; \qquad t = T\,\frac{2\pi^2}{\hbar\omega}\,. \tag{34}$$

Expanding for large temperatures and using $\hbar\omega \propto N^{-1/3}$, this gives, indeed, a temperature suppression factor $\propto \exp(-N^{1/3})$. Therefore, Pedersen *et al.* (1991) in the analysis of their spectacular experiments multiplied the logarithmic derivatives of the mass yields I_N by $\sqrt{N}\exp(cN^{1/3})$, where c is a constant containing an effective temperature, and the root factor compensates the decrease of the shell correction at $T = 0$ with increasing N (Bohr and Mottelson, 1975).

We refer to Bjørnholm's lectures for the details of this analysis and of its results in which the super-shell structure has, indeed, been put into evidence experimentally for the first time. In Figure 5, we have copied the relevant figure of Pedersen *et al.* (1991) and compare it to the theoretical KS results by Genzken and Brack

(1991). Here the negative second difference $-\Delta_2 F(N)$ is shown, multiplied by the same enhancement factor (with the value of c readjusted by $\sim$ 10%). Although the assumption $-\Delta_2 F(N) \propto \Delta_1 \ln I_N$ is a very crude one (see Bjørnholm *et al.*, 1991, for a discussion on this point), the agreement of the two curves is striking. This demonstrates that the *finite temperature of the valence electrons* which alone contribute to the quantities shown here — the ionic parts of the free energies cancel in the differences $\Delta_2 F(N)$ and $\Delta_1 \ln I_N$ — plays an essential role in the mass yields and can be correctly taken into account in selfconsistent KS calculations even in the simple jellium model. No need to stress that no other, i.e. more structural, model will ever be used to calculate the super-shells in such large systems!

REFERENCES

Andreoni, W., 1991, Z. Phys. D 19, 31

Ashcroft, N.W., Mermin, N.D., 1976, *Solid State Physics* (Holt-Saunders Intern. Editions)

Balbàs, L.C., Rubio, A., 1991, Ann. Phys. (Spain) in print

Balian, R., Bloch, C., 1971, Ann. Phys. (N. Y.) 69, 76

Beck, D.E., 1984a, Solid State Commun. 49, 381

Beck, D.E., 1984b, Phys. Rev. B 30, 6935

Bertsch, G., 1990, Comput. Phys. Commun. 60, 247

Bertsch, G.F., Tomanek, D., 1989, Phys. Rev. B 40, 2749

Bjørnholm, S., Borggreen, J., Echt, O., Hansen, K., Pedersen, J., Rasmussen, H.D., 1991, Z. Phys. D 19, 47

Bohr, A., Mottelson, B.R., 1975, *Nuclear Structure II* (Benjamin)

Bréchignac, C., Cahuzac, Ph., Leygnier, J., Pflaum, R., Roux, J.Ph., Weiner, J., 1989, Z. Phys. D 12, 199

Brack, M., 1989, Phys. Rev. B 39, 3533

Brack, M., Quentin, P., 1981, Nucl. Phys. A 361, 35

Brack, M., Genzken, O., Hansen, K., 1991a, Z. Phys. D 19, 51

Brack, M., Genzken, O., Hansen, K., 1991b, Z. Phys. D 21, 65

Car, R., and Parrinello, M., 1985, Phys. Rev. Lett. 55, 2471

Cini, M., 1975, J. Catal. 37, 187

de Heer, W.A., Brack, M., 1992, review article in preparation for Rev. Mod. Phys.

de Heer, W.A., Selby, K., Kresin, V., Masui, J., Vollmer, M., Chatelain, A., Knight, W.D., 1987a, Phys. Rev. Lett. 59, 1805

de Heer, W.A., Knight, W.D., Chou, M.Y., Cohen, M.L., 1987b, Solid State Physics 40, 93

Dreizler, R., Gross, E.K.U., 1990, *Density Functional Theory* (Springer, Berlin)

Ekardt, W., 1984a, Phys. Rev. Lett. 52, 1925

Ekardt, W., 1984b, Phys. Rev. B 29, 1558

Ekardt, W., 1985a, Phys. Rev. B 31, 6360

Ekardt, W., 1985b, Phys. Rev. B 32, 1961

Ekardt, W., 1986, Phys. Rev. B 34, 526

Ekardt, W., Penzar, Z., 1988, Phys. Rev. B 38, 4273

Ekardt, W., Penzar, Z., 1991, Phys. Rev. B 43, 1322

Engel, E., Perdew, J.P., 1991, Phys. Rev. B 43, 1331

Evans, R., 1979, Adv. in Phys. 28, 143

Fermi, E., 1928, Z. Phys. 48, 73

Genzken, O., Brack, M., 1991, Phys. Rev. Lett., in print

Gilbert, T.L., 1975, Phys. Rev. B 12, 2111

Guet, C., Johnson, W.R., 1991, Preprint C.E.N.G. - DRFMC/SPHAT

Gunnarsson, O., Lundqvist, B.I., 1976, Phys. Rev. B 13, 4274

Gupta, U., Rajagopal, A.K., 1982, Physics Reports 87, 259

Hill, D.L., Wheeler, J.A. , 1953, Phys. Rev. 89, 1102

Hohenberg, P., Kohn, W., 1964, Phys. Rev. 136, B864

Iñiguez, M.P., Lopez, M.J., Alonso, J.A., Soler, J.M., 1989, Z. Phys. D 11, 163

Jones, R.O., 1991, Phys. Rev. Lett. (in print)

Jones, R.O., Gunnarsson, O., 1989, Rev. Mod. Phys. 61, 689

Kirkpatrick, S., Gelatt, C.D., and Vecchi, M.P., 1983, Science 220, 671

Kohn, W., Sham, L.J., 1965, Phys. Rev. 140, A1133

Koutecký, J., *et al.*, 1991, J. Chem. Phys. , in print

Lang, N.D., Kohn, W., 1970, Phys. Rev. B 1, 4555

Lang, N.D., Kohn, W., 1971, Phys. Rev. B 3, 1215

Lang, N.D., Kohn, W., 1973, Phys. Rev. B 7, 3541

Lauritsch, G., Reinhard, P.-G., Meyer, J., Brack, M., 1991, Phys. Lett. A, in press

Levy, M., 1979, Proc. Natl. Acad. Sci. (USA) 76, 6062

Levy, M., Perdew, J.P., 1985, Phys. Rev. A 32, 2010

Manninen, M., 1986, Phys. Rev. B 34, 6886

Martins, J.L., Car, R., Buttet, J., 1981, Surf. Sci. 106, 265

Mermin, N.D., 1965, Phys. Rev. 137, 1441A

Mie, G., 1908, Ann. Phys. (Leipzig) 25, 377

Monnier, R., Perdew, J.P., Langreth, D.C., Wilkins, J.W., 1978, Phys. Rev. B 18, 656

Myers, W.D., Swiatecki, W.J., 1969, Ann. Phys. (N.Y.) 55, 395

Nishioka, H., Hansen, K., Mottelson, B.R., 1990, Phys. Rev. B 42, 9377

Pedersen, J., Bjørnholm, S., Borggreen, J., Hansen, K., Martin, T.P., Rasmussen, H.D., 1991, Preprint NBI-91-22, submitted to Nature

Penzar, Z., Ekardt, W., 1990, Z. Phys. D 17, 69

Perdew, J.P., Zunger, A., 1981, Phys. Rev. B 23, 5048

Röthlisberger, U., Andreoni, W., 1991, Z. Phys. D 20, 243

Reinhard, P.-G., Brack, M., Genzken, O., 1990, Phys. Rev. A 41, 5568

Seidl, M., Meiwes-Broer, K.-H., Brack, M., 1991, J. Chem. Phys. 95, 1295

Selby, K., Vollmer, M., Masui, J., Kresin, V., de Heer, W.A., Knight, W.D., 1989, Phys. Rev. B 40, 5417

Selby, K., Kresin, V., Masui, J., Vollmer, M., de Heer, W.A., Scheidemann, A., Knight, W.D., 1991, Phys. Rev. B 43, 4565

Serra, Ll., Garcias, F., Barranco, M., Navarro, J., Balbas, C., Mañanes, A., 1989, Phys. Rev. B 39, 8247

Serra, L., Garcias, F., Barranco, M., Barberan, N., Navarro, J., 1990, Phys. Rev. B 41, 3434

Snider, D.R., Sorbello, R.S., 1983, Phys. Rev. B 28, 5702

Thomas, L.H., 1927, Proc. Cambr. Philos. Soc. 23, 542

Tiggesbäumker, J., Köller, L., Lutz, H.O., Meiwes-Broer, K.-H., 1991, XIII. International Symposium on Molecular Beams, El Escorial, Spain; and to be published

Yannouleas, C., Broglia, R.A., Brack, M., Bortignon, P.F., 1989, Phys. Rev. Lett. 63, 255

FIGURE CAPTIONS

Figure 1:

Variational densities $\rho(r)$ (in units of ρ_{I0}) and selfconsistent total potentials $V(r)$ for the neutral Na_{198} cluster ($r_s = 4.0$). Solid lines: KS results by Ekardt (1984b). Dash-dotted and dashed lines: semiclassical results using the functional $\tau_{ETF}[\rho]$ up to 2nd and 4th order in $\hbar$, respectively, by Brack (1989).

Figure 2:

Energies of surface plasmons of multipolarity L for spherical Na clusters versus jellium radius R_I. Solid lines: RPA sum-rule approximation $\hbar\omega_L = \sqrt{m_3/m_1}$ in terms of Tassie operators $Q_L = r^L Y_{L0}$ ($L \neq 0$) and $Q_0 = r^2$ ($L = 0$). Dashed lines: centroid of collective spectrum obtained in "local RPA" (see text). All quantities evaluated in terms of semiclassical ETF densities (Brack, 1989). On the right margin: classical Mie frequencies.

Figure 3:

Potential energy surface of Na_{12} (equidistance 0.01 Ry for dashed and 0.05 Ry for full lines) in the β, γ plane. The minimum at $\beta = 0.54$, $\gamma = 15^o$ is at -1.768 Ry (Lauritsch *et al.*, 1991).

Figure 4:

Free energy shell-correction $\delta F(N) = F(N) - F_{LDM}(N)$ for spherical Na clusters versus $N^{1/3}$ for three different temperatures T, obtained in selfconsistent KS calculations (Genkzen and Brack, 1991). LDM parameters used at $T = 0$ K: $a_s = 0.6259$, $a_c = 0.2041$; at $T = 400$ K: $a_s = 0.5918$, $a_c = 0.3796$; and at $T = 600$ K: $a_s = 0.5755$, $a_c = 0.4204$ (all in eV). Numbers near the bottom are the magic numbers of filled major spherical electronic shells.

Figure 5:

Upper part: Relative variation $< \Delta_1 \ln I_N >_{K_0}$ in experimental Na cluster abundance I_N versus $N^{1/3}$ (Pedersen *et al.*, 1991; see this reference for the details). *Lower part:* Negative second difference $-\Delta_2 F(N)$ of free energy obtained in selfconsistent KS calculations at $T = 600$ K (Genzken and Brack, 1991). Both quantities are enhanced by a N-dependent factor to compensate for the temperature suppression (see text).

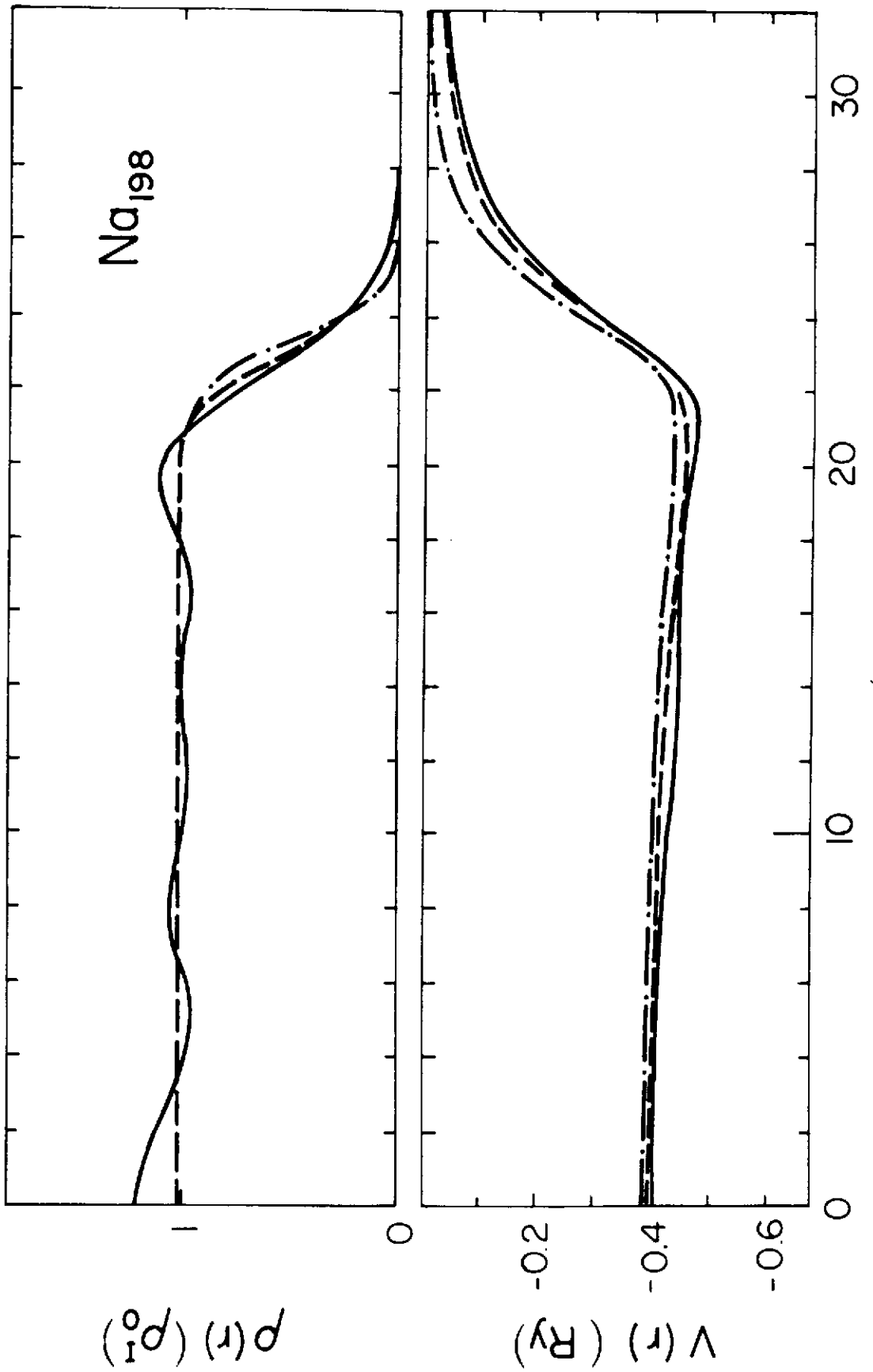

Figure 1

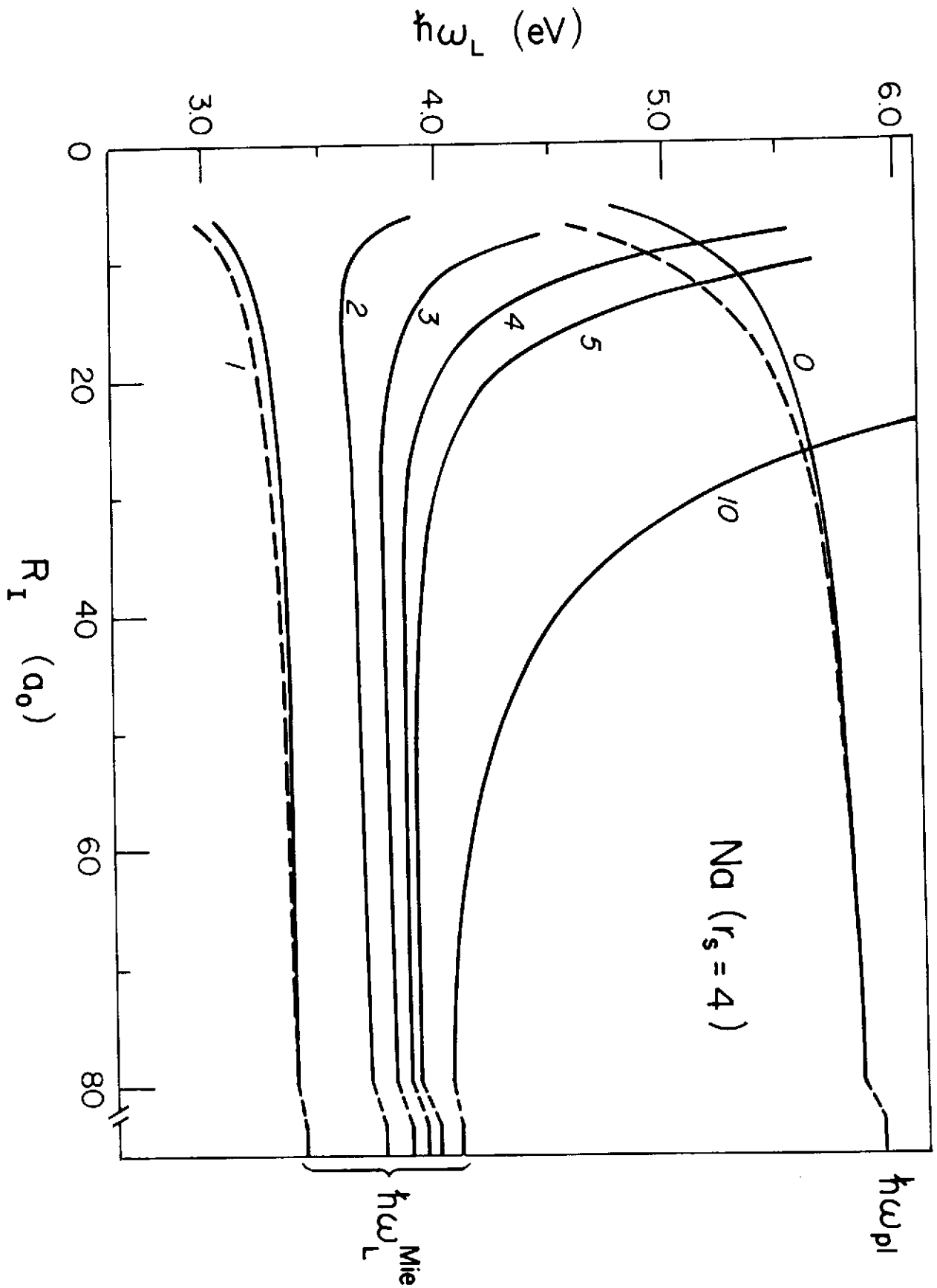

Figure 2

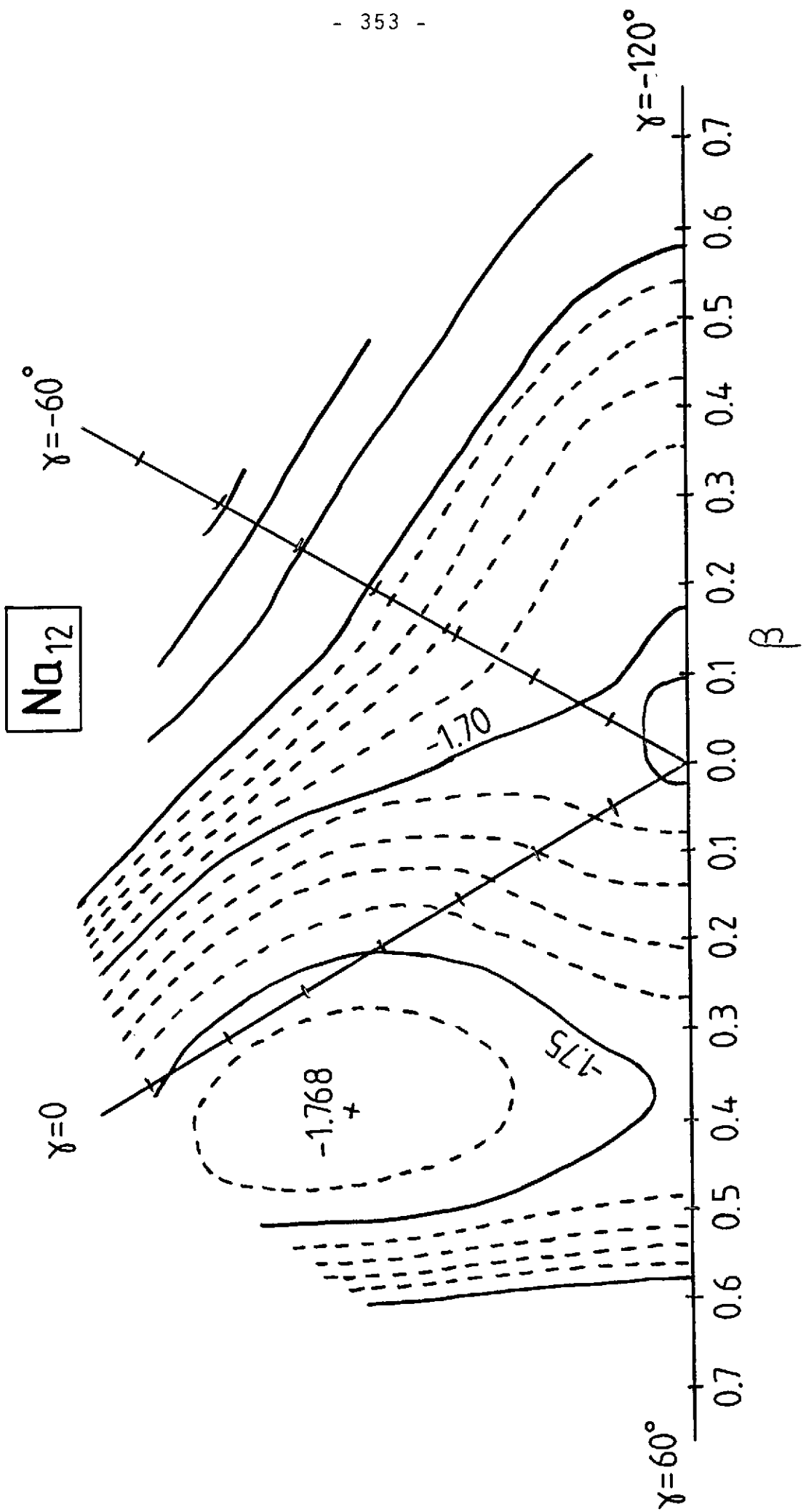

Figure 3

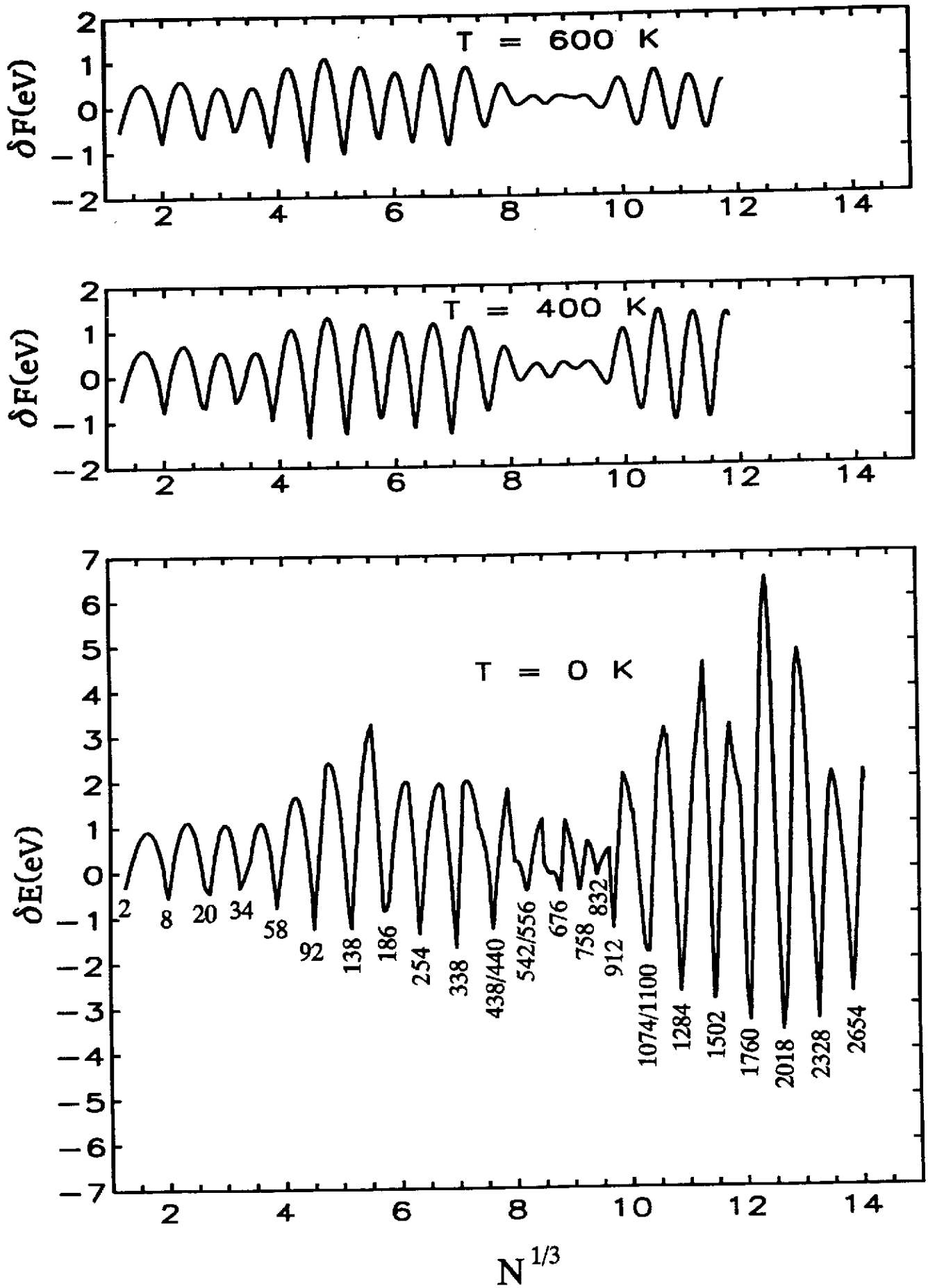
T = 600 K
δF(eV)
T = 400 K
δF(eV)
T = 0 K
δE(eV)
2
8
20
34
58
92
138
186
254
338
438/440
542/556
676
758
832
912
1074/1100
1284
1502
1760
2018
2328
2654
N 1/3

Figure 4

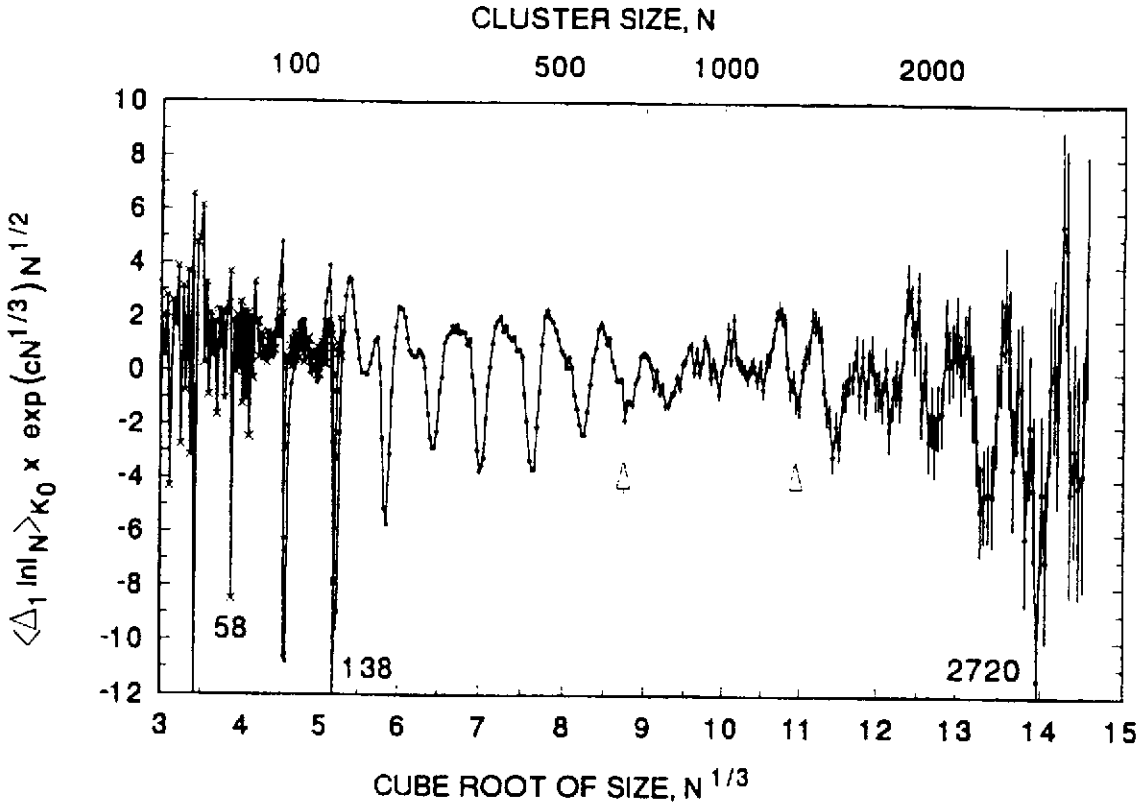
CLUSTER SIZE, N
100
500
1000
2000
$\langle \Delta_1 \ln I_N \rangle_{K_0} \times \exp(cN^{1/3}) N^{1/2}$
58
138
2720
CUBE ROOT OF SIZE, $N^{1/3}$

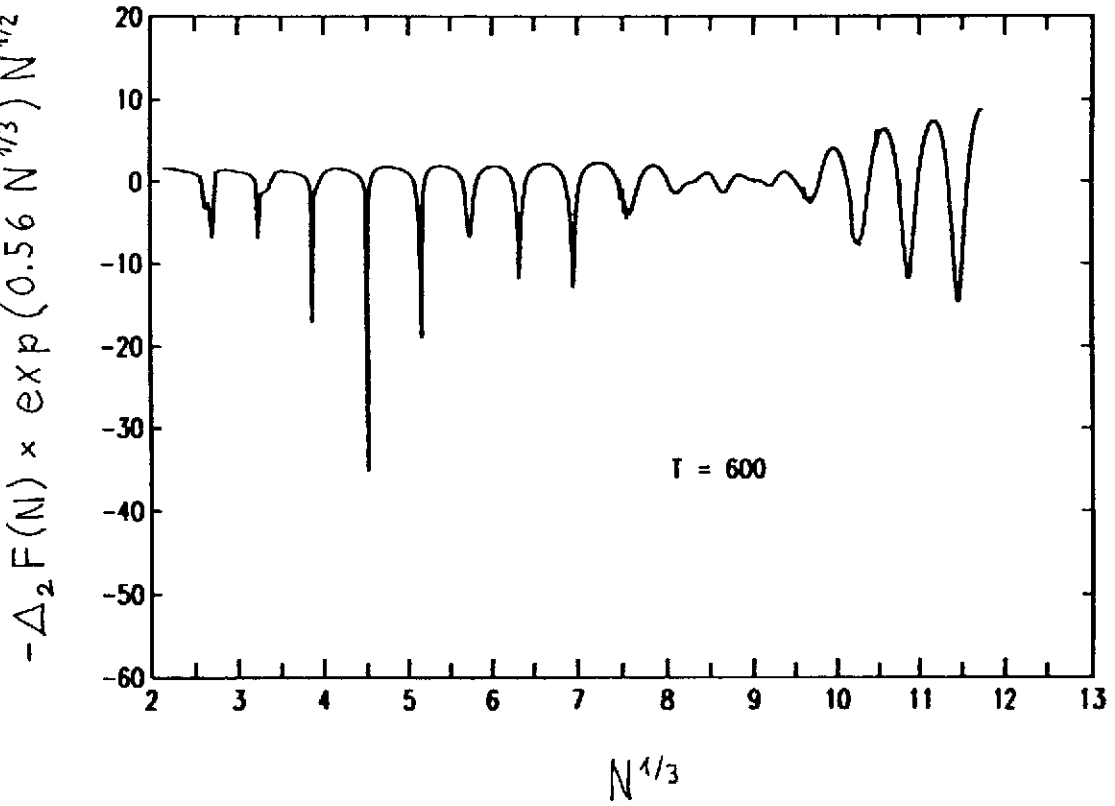
$-\Delta_2 F(N) \times \exp(0.56\, N^{1/3})\, N^{1/2}$
T = 600
$N^{1/3}$

Figure 5